OVERVIEW OF HIGH INTENSITY X-RAY AND GAMMA-RAY SOURCES

K. R. Prestwich, J. R. Lee, J. J. Ramirez, and T. W. L. Sanford
Sandia National Laboratories
Albuquerque, NM 87185

F. J. Agee
Harry Diamond Laboratories
Adelphi, MD 20783

G. B. Frazier
Physics International Company
San Leandro, CA 94577

A. R. Miller
Maxwell Laboratories, Incorporated
San Diego, CA 92123

Abstract

The requirements for intense x-ray and gamma-ray sources to simulate the radiation effects from nuclear weapons has led to the development of several types of terawatt-pulsed power systems. One example of a major gamma-ray source is Aurora, a 10-MV, 1.6-MA, 120-ns four-module, electron-beam generator. Recent requirements to improve the dose rate has led to the Aurora upgrade program and to the development of the 20-MV, 800-kA, 40-ns Hermes-III electron-beam accelerator. The Aurora program includes improvements to the pulsed power system and research on techniques to improve the pulse shape of the electron beam. Hermes III will feature twenty 1-MV, 800-kA induction accelerator cavities supplying energy to a magnetically insulated transmission line adder. Hermes III will become operational in 1988. Intense x-ray sources consist of pulsed power systems that operate with 1-MV to 2-MV output voltages and up to 25-TW output powers. These high powers are achieved with either low impedance electron-beam generators or multimodular pulsed power systems. The low-impedance generators have high voltage Marx generators that store the energy and then sequentially transfer this energy to pulse-forming transmission lines with lower and lower impedance until the high currents are reached. In the multimodule machines, each module produces 0.7-TW to 4-TW output pulses, and all of the modules are connected together to supply energy to a single diode.

Introduction

High intensity x-ray and gamma sources are used to simulate the effects of radiation from a nuclear weapon.[1,2] In order to produce the radiation dose with bremsstrahlung radiation, very high peak power electron-beam generators are required. The x-rays are usually produced with 1-MeV to 2-MeV electron beams and gamma rays with 10-MeV to 20-MeV electrons. Since the voltage is fixed by spectrum considerations, efforts to increase the dose rate result in requirements for higher beam current, implying lower impedance generators. Since bremsstrahlung production efficiency scales almost linearly with voltage, the need to obtain low impedances is much greater in x-ray generators than gamma-ray generators. The pulse rise time, that is determined by switching techniques and diode inductance, limited the pulse durations to 50 ns to 150 ns in early machines. Recent developments have allowed the potential for 20-ns to 50-ns pulse durations. In this paper the evolution of both types of simulators are traced with indications of the technology improvements that allowed the progress to occur. The next section covers gamma-ray simulators with descriptions of Aurora, including recent improvements, and of Hermes III, a 20-MV, 800-kA, 40-ns accelerator that will be completed in 1988. This will be followed by descriptions of three types of x-ray generation machines: a) single stage, b) multiple stages in series, and c) multiple module machines.

Gamma-Ray Simulators

The Aurora machine[3,4] was developed by Physics International for the Defense Nuclear Agency (DNA) to supply a uniform radiation dose over a large volume. This electron-beam accelerator produces four 12-MV, 400-kA, 125-ns electron beams. It has four, 20-Ω, 125-ns PFL Blumleins that are 7 m in diameter and configured as shown in Fig. 1. The pulses from these PFLs are synchronized within 20 ns to produce the desired radiation pulse. This synchronization is achieved with three-electrode, triggered, oil-dielectric spark gaps that produce 4 to 6 arcs on each

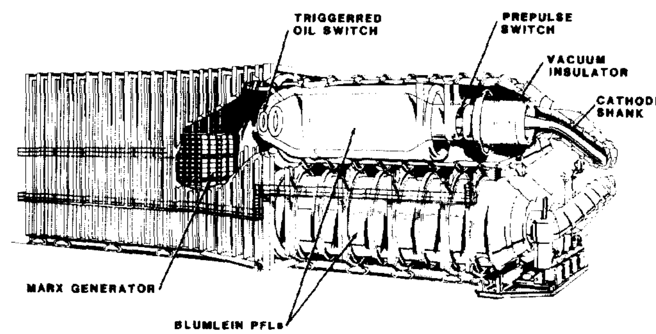

Fig. 1. Aurora, a 12-MV, 1.6-MA, 125-ns electron-beam accelerator. This machine has four Marx generators, four Blumlein PFLs and four electron-beam diodes.

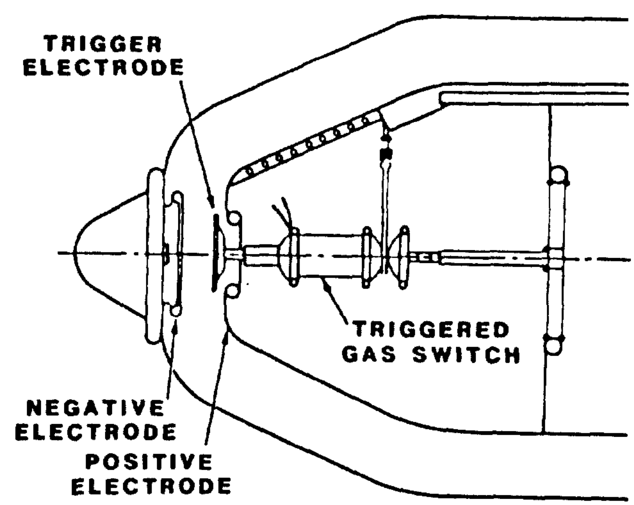

Fig. 2. The 12-MV, multichannel, oil-dielectric spark gap on the Aurora Blumleins. The switch consists of two main electrodes labeled positive and negative and one sharp-edged trigger electrode.

closure. The trigger electrode is a sharp-edged disk that is located about 17% of the main electrode distance from the ground electrode, as shown in Fig. 2. It is capacitively biased such that there is only a small enhancement of the mean electric field at the edges of the disk during charging of the PFLs. The gas switch is a SF_6-insulated spark gap that can be triggered by a 200-kV pulse. When the gas switch closes, the voltage polarity on the trigger disk reverses in about 200 ns. This reversal time is determined by the disk capacitance and the circuit inductor. This change in voltage on the trigger disk and the large field enhancement on the disc edge results in closure of 4 to 6 channels with a 10-ns rms jitter. With the multi-channels, this switch can carry the 1-MA current and produce the desired pulse rise time.[3,4]

Each Aurora module has a magnetically insulated transmission line (MITL) that allows the four anode-cathode gaps and bremsstrahlung converters to be near one another so that the gamma rays from the four modules overlap in the test volume.

An improvement program is underway to reduce maintenance requirements and to allow better control of the output pulse waveform. New Marx generators are being designed. An improved trigger scheme for the Blumlein oil switches, that could reduce their jitter to 4 ns, is being developed. Diverter switch networks have been developed that will allow a variable pulse width by crowbarring the output pulse through a resistor.[5]

The lower jitter switching can be accomplished by applying a high-voltage trigger pulse that rises in ~20 ns rather than the 200 ns reversal in the present switches. A large fast-rising trigger pulse can substantially reduce the closure time of the wide gap. If the trigger pulse amplitude is too large, the narrow side of the gap will close first and the driving voltage for the wide side drops to V_0, implying a longer closure time. Therefore there is an optimum trigger voltage for a fixed gap spacing that will give a minimum closure time. For the Proto-I experiments, jitter was 4% of the closure time.[6] Experiments are underway to develop an appropriate 5-MV to 6-MV trigger generator and to expand the streamer velocity data base. A decision on implementation of such a system will be made following these experiments.

Since the inductance of the vacuum insulator stack limits the pulse rise time even if the number of switch channels is significantly improved, techniques for sharpening the gamma-ray pulse rise time are being explored. One promising technique under consideration is to erode away the front of the electron-beam pulse by propagating the beam in a gas prior to impact on the converter.[7]

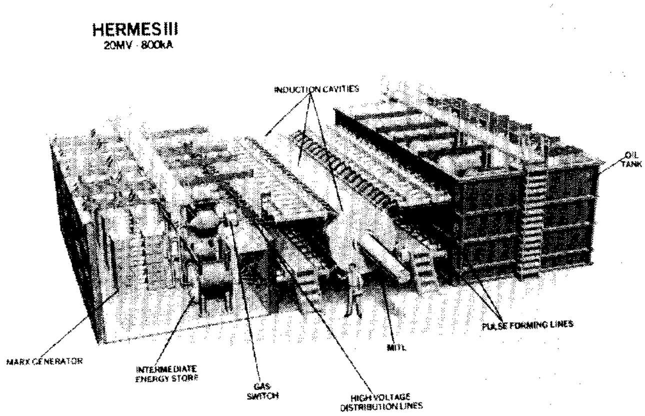

Fig. 3. Hermes III, a 20-MV, 800-kA, electron-beam accelerator

A new gamma-ray simulator, Hermes III, is being developed at Sandia National Laboratories that will provide 5×10^{12} rad/s dose rates. Hermes III is designed to produce a 20-MV, 800-kA, 40-ns electron beam. Figure 3 is a sketch of this accelerator. The major subsystems in this accelerator are ten Marx generators, twenty intermediate storage capacitors, twenty laser-triggered, 2-MV spark gaps, eighty 1-MV pulse-forming transmission lines, and twenty induction cavities that feed energy to a MITL adder network. The MITL supplies energy to a cold-cathode, indented-anode electron-beam diode.

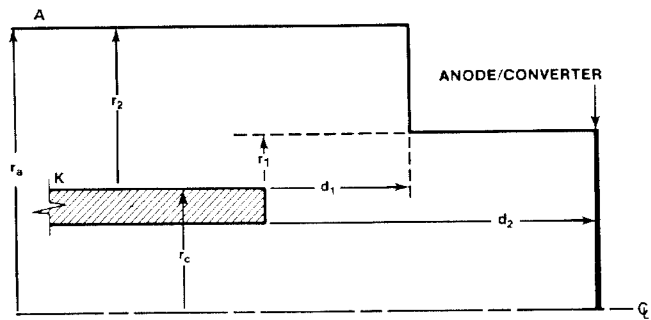

Fig. 4. Diagram of indented-anode diode

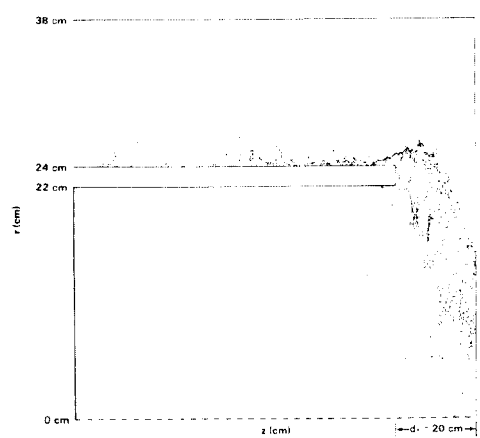

Fig. 5(a). MAGIC simulation of MITL/diode with a 20-cm AK Gap: V = 18 MV, 1 = 0.8 MA, Z = 23 Ω, θ = 49° ± 10°.

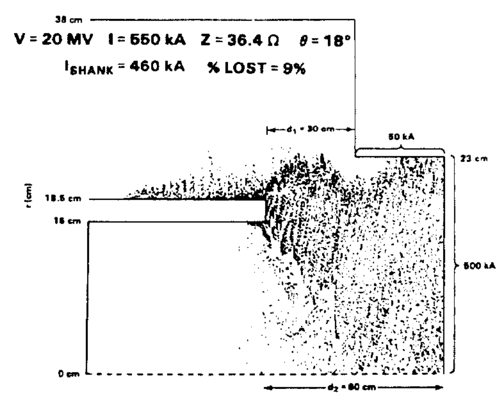

Fig. 5(b). V = 20 MV, I = 550 kA, Z = 36 Ω, and $\bar{\theta}$ = 18° ± 7°.

A sketch of this indented anode diode is shown in Fig. 4. Calculated electron-beam trajectories for a standard electron-beam diode and an indented anode diode are shown in Figs. 5(a) and 5(b) respectively.[8] Figure 5(a) indicates that in a standard diode, the beam pinches due to the self-magnetic fields of the beam and the reduction of the radial electric fields of the beam due to the presence of the metal anode. This pinch results in an average angle of incidence of the electrons at the anode, θ, equal to about 49°. With $\theta = 49°$, a uniform radiation dose over a reasonable volume can not be produced. If part of the anode is relocated, as shown in Fig. 4, the radial electric field due to the space charge returns at the previous anode position and simulations show that θ can be reduced to ~14° without excessive loss of electrons to the cylindrical portion of the anode. With $\theta \sim 14°$, a uniform radiation dose over the desired volume can be achieved.

The induction cavities and MITL adder are patterned after those successfully demonstrated in the 4-MV, 250-kA Helia experiment.[9] Figure 6 is a schematic drawing of the MITL adder. If the output impedance of each cavity is Z_1, the MITL impedance must increase from Z_1 to 20 Z_1 in steps as it passes through the twenty cavities. For example, the wave coming from cavity 1 with an amplitude V_0 on an MITL with impedance Z_1 is effectively in series with output of cavity 2 with impedance Z_1 and voltage V_1. These two feed a matched MITL load 2 Z_1, and a forward going wave of 2 V_0 results. In similar fashion the voltage builds up to 20 V_0 across an MITL impedance of 20 Z_1 at the 20th cavity.

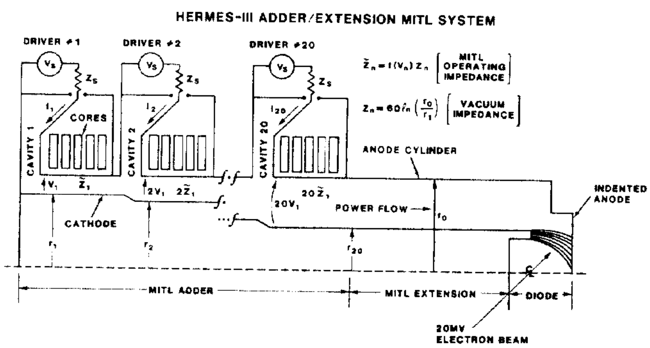

Fig. 6. Schematic diagram of Hermes-III MITL adder and MITL extension

The cavities are inductively isolated, as indicated in Fig. 6. Similar to Helia, these cavities are designed with azimuthal transmission line mixing circuits to symmetrize the current flow to the MITL adder, independent of the spread in arrival time of the four input pulses to the cavities.[9]

The four PFLs are operated in parallel and act as current adders. Each line supplies a nominal 1.1-MV, 220-kA pulse to the cavity to give a 1.0-MV, 800-kA cavity output pulse. Each water dielectric PFL is 5 Ω and is charged to 2.2 MV in 220 ns. Single-channel, water-dielectric spark gaps close with less than 3-ns rms jitter. The pulse rise time will be improved with a water-dielectric peaking switch. A crowbar switch will be used to control the width of the pulse.

The initiation of the charge of the PFL is controlled by laser-triggered spark gaps. The jitter of these gaps has been measured to be less than 2 ns with ~10 mJ of laser energy focused in the trigger gap of these multistage switches. Each 2.4-MV Marx generator is essentially identical to two rows of a PBFA-II Marx generator.[10] Testing of the Hermes-III pulsed power system through the PFLs will start in April. Installation of the cavities will be done in the fall with testing of the full accelerator scheduled for approximately one year from now.

Intense X-Ray Sources

Since the electron-beam energy for these sources is limited to 1-MeV to 2-MeV by requirements on the photon spectrum, single-stage generators with low output impedance were developed and two different paths were pursued to improve the x-ray dose. The single-stage, pulse-forming devices with 2-4 Ω water dielectric coaxial transmission lines are represented by such machines as Hydra,[11] Owl,[12] Gamble II,[13] and BLACKJACK 2.[14] The BLACKJACK 2 is described in the following paragraph as a representation of this type of machine. This description is followed by a discussion of BLACKJACK 3, BLACKJACK 5, and BLACKJACK 5' to show the evolution of the accelerators with multiple stages in series. This accelerator development was sponsored by DNA.

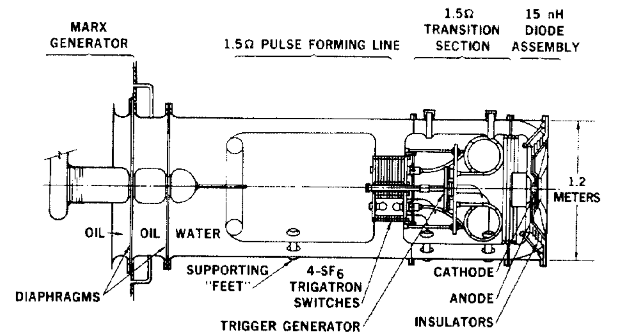

Fig. 7. BLACKJACK 2, 1.5 Ω electron-beam accelerator. Output power, 0.6 TW

One of the earliest pulsers produced at Maxwell Laboratories was BLACKJACK 2 (Fig. 7). This machine had an output impedance of 1.5 Ω and delivered almost 30 kJ in an electron beam. It featured a pulse-forming line charged directly by a Marx generator to 2 MV. Output switching was by four command triggered, gas dielectric, trigatrons in parallel. These had graded plastic envelopes to separate SF_6 at 100 psi from the water. The first to last closure scatter of these switches was characterized by a σ of 5 ns. An effective inductance of 80 nH gave 30-ns rise times. Further inductance reduction was limited by the small number of switches which could be put in parallel. This fact and the triggering complexity motivated the change of emphasis to switching directly in water.

The advantage of this scheme is that it can be utilized to produce low inductance switches in pulsers of large dimensions. Instead of locating a single switch on the axis of a pulser, with a large inductance resulting from the current convergence, the sites can be distributed around the perimeter of a given coaxial stage.

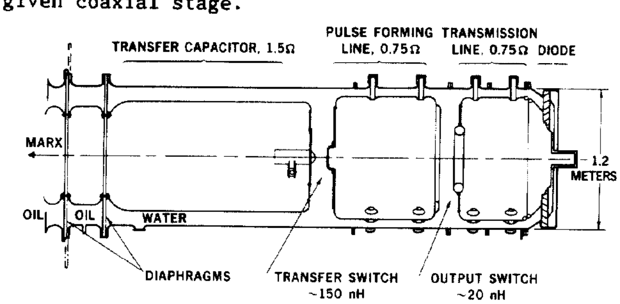

Fig. 8. A cross-section of the 3/4-Ω, 1.3-TW BLACKJACK 3 pulse line

The above notions were used in 1974 on BLACKJACK 3 (Fig. 8). This machine delivers about 40 kJ in a 60-ns pulse. Peak output power is 1.3 TW at a peak current slightly over 1 MA. This pulser operated on a routine basis with a twelve-channel, self-closing, multi-site, water dielectric output switch. Inductance was 20 nH at 2 MV. The single-channel transfer switch is also a self-closing water switch with an inductance of 150 nH at 2.25 MV. The transfer capacitor is needed to charge the pulse-forming line rapidly enough for proper operation of the output switch. These improvements doubled the power without an increase in size.

This type of machine culminated with the development of BLACKJACK 5.[14,15] BLACKJACK 5 is 4 m in diameter and about 10-m long. The schematic view in Fig. 9 shows the pulse-line structure in cross section and illustrated the number of stages used to produce power gain. These stages are interconnected by self-closing water switches. Between the first and second stage is a single-channel switch. The remaining stages are connected by six 16- and 32-channel switches with respective inductances of 80 nH, 30 nH, and 10 nH. Peak stage voltages at the 10-TW level are 5.7 MV, 5.2 MV, 4.9 MV and 3.9 MV with charge times per stage of 1700 ns, 500 ns, 170 ns and 70 ns, respectively. The largest electrode areas are $>0.5 \times 10^6$ cm^2. Two design features are implicit in this construction. The first is the large annular plastic diaphragms which support and insulate the stages. These operate at essentially the same electrical stress as the water. The second point is that pulse width variations are obtained by closing selected switches prior to operation. This can result in the output pulse being produced by either a 50-ns, a 100-ns, or a 150-ns pulse-forming line. For example: closure of the 32-channel switch connects the 25-ns PFL as a part of the transmission line and the 16-channel switch then acts as an output switch for the 50-ns IPFL. The times shown are one way transit times. This flexibility was called for in optimizing load design and has proven useful.

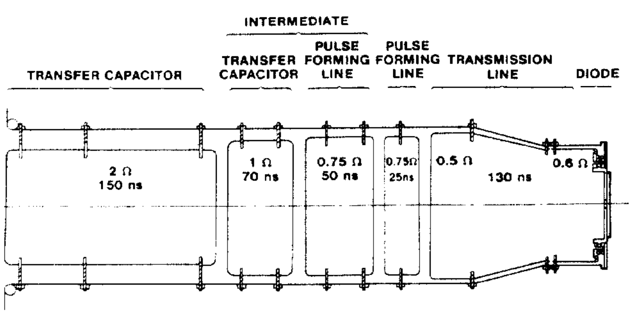

Fig. 9. Cross-sectional view of the BLACKJACK 5 pulse line

That the energy storage and power flow in this pulse line is confined to a narrow annular region is clearly shown in Fig. 9. Power gain is achieved through sequential transfer of energy from stage-to-stage in progressively shorter times. Energy is stored transiently in, and power flow is through, annular regions at the large radii that are required for breakdown free operation at high voltage and low impedance. Consequently, much of the internal volume goes unused. Self-closing multi-channel switches are used at each stage.

Additional energy can be stored, and a second parallel path for power flow established in the interior of this pulser structure, provided there is some means for coupling the two separate pulsers thus formed. Ground plane shielded switching,[16] provides the means for accomplishing this. These internal additions are the basis for BLACKJACK 5′ and are shown in Fig. 10.

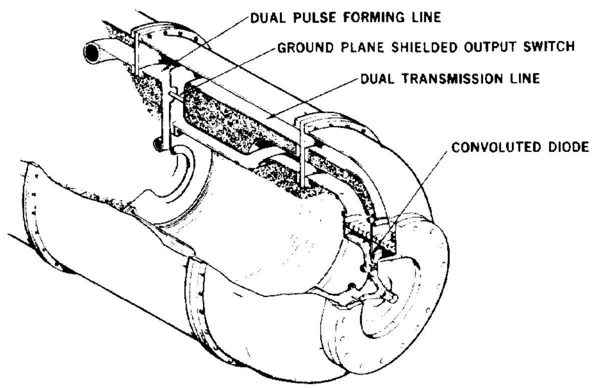

Fig. 10. Cross section of BLACKJACK 5′ modification

The output section of BLACKJACK 5 has been modified as shown. Two parallel output transmission lines were installed, the inner being slightly higher impedance, giving a net parallel impedance of 0.3 Ω. Driving this is a folded pulse-forming line stage that is half-coaxial, half-radial transmission line. As charged by the previous stage, this is a 100-ns, 0.75-Ω line.

When switched in the middle, its output impedance is reduced to ~0.4 Ω, and it delivers a 50-ns pulse to the dual transmission lines. The ground plane through the switch region ensures continuity of current flow on the inner ground conductors.

As the impedance gets lower, a smaller portion of the large cylindrical volume is used to store energy. This observation led to the development of modular strip-transmission line generators, such as Proto II,[17] Double-EAGLE,[18] and Saturn.

Double-EAGLE, a 7-TW simulator built for the DNA, became operational in November 1983. Double-EAGLE consists of two EAGLE modules[19] feeding a common vacuum region (Fig. 11). The two types of loads routinely fielded on Double-EAGLE are imploding plasmas for production of soft x-rays (<4.0 keV) and electron-beam diodes for production of harder x-rays (<1 MeV).

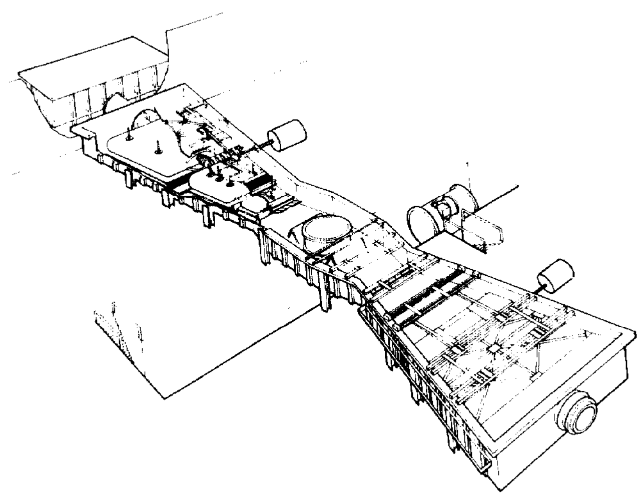

Fig. 11. Sketch of the Double-EAGLE machine

Each of the two EAGLE modules consists of a Marx generator, transfer capacitor (TC), a triggered gas switch, a charging pulse line, two sets of water switches, and an output line (OL). The two output lines are terminated at a common circular tube (vacuum-water interface) and connected to the load through magnetically insulated, vacuum transmission lines (MITL). The voltages measured along an EAGLE module are shown in Fig. 12, with the module terminated in a fixed resistor load. It is important to note from Figs. 11 and 12 that Double-EAGLE is a triplate machine with an upper and lower ground plane.

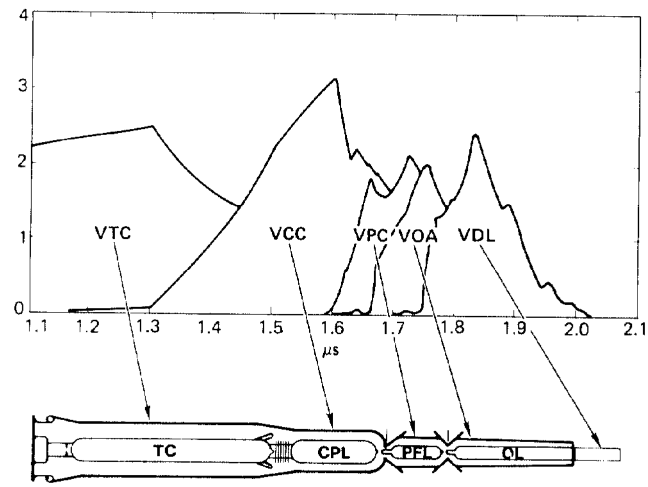

Fig. 12. Voltage Waveforms for each EAGLE module

Each Double-EAGLE Marx stores 590 kJ at ±60 kV/stage. The nominal 6.5-TW operating level is at ±60 kV on the Marxes, with a maximum Marx charge of ±75 kV. Each Marx generator charges two 100-nF TC lines to about 2.5 MV in 1.3 μs.

Two externally triggered gas switches are used to synchronize the EAGLE modules. The Double-EAGLE switches have eight, SF_6-insulated stages with one of the eight stages electrically triggered. Once the gas switches are triggered, the CPLs charge in about 350 ns. The CPL an PFL are both discharged through self-breaking water switches. These water switches have discrete field-enhanced multiple electrodes.

The final transformer, or OL, is charged in 95 ns by the second set of water switches. The final impedance of the OL is 0.5 Ω. The OL terminates in transit-time equalizer bumps.[18] The purpose of these bumps is to improve the azimuthal uniformity of the current delivered to the tube and magnetically insulated vacuum feeds.

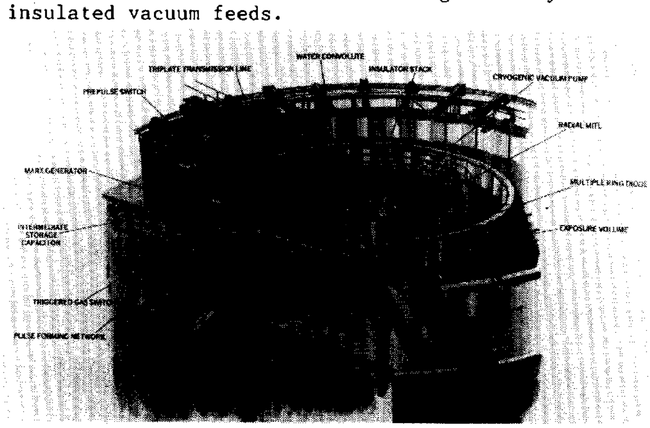

Fig. 13. Drawing of Saturn, a 2-MV, 25-TW electron-beam accelerator

Proto II is a 1.5-MV, 5.5-MA electron-beam generator with either a 20 or 50 ns output pulse.[20] Proto II provided the technology for the design of Saturn, a 2-MV, 25-TW accelerator, now under construction at Sandia National Laboratories. This accelerator is a rebuild of the PBFA-I accelerator.[21] Saturn will have 36 independent modules supplying energy to the unique electron-beam diode. A sketch of this accelerator is shown in Fig. 13. Each 3-MV Marx generator charges an intermediate storage capacitor to about 2.5 MV. The intermediate storage capacitor charges two triplate, water-dielectric transmission lines in ~300 ns. Self-closing, water-dielectric spark gaps initiate the energy transfer from each PFL to the transmission lines. A 2:1 mismatch impedance at that point produces a 1.6-MV forward-going wave. The wave is transmitted through a parallel plate transmission line transformer with the impedance varying from 2.0-Ω to 2.4-Ω and a 2.4 Ω impedance triplate line. This triplate connects to two pipe-plane transmission line transformers (2.4 Ω to 4.2 Ω).

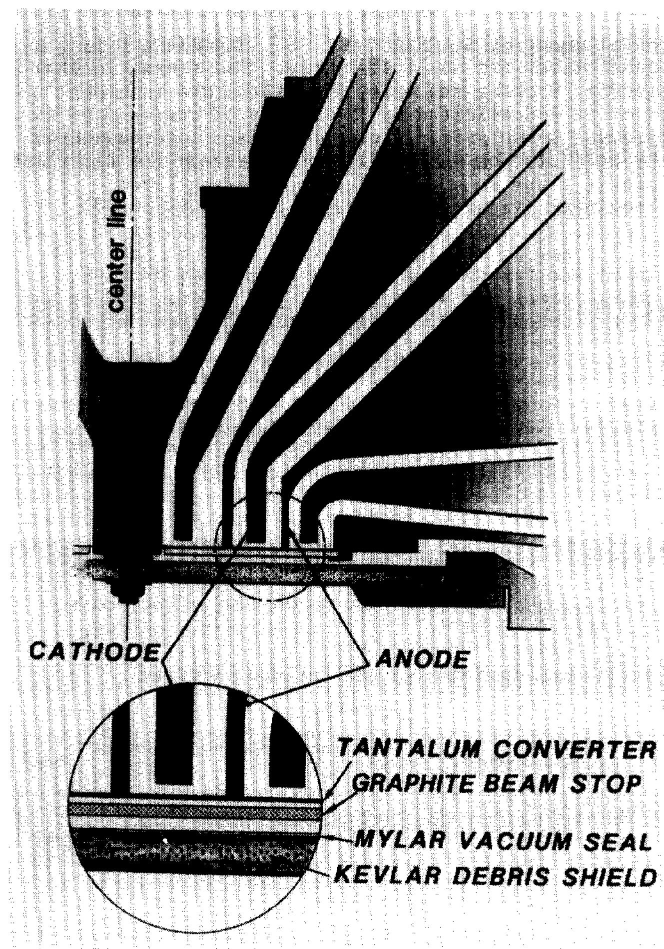

Fig. 14. Saturn ring diode

The output of these 72 transmission line transformers is fed to the insulator stack and three conical vacuum transmission lines that transmit the 2-MV pulses to the electron-beam diode. The diode consists of three independent ring cathodes and anodes,[22] as shown in Fig. 14. The number of the 4.1-Ω transmission lines that feed each section is varied to provide a constant linear current density at each of the three anodes. At 2 MV, 12 MA these diodes should produce 5×10^{12} rads/s over a 500 cm^2 area.

Acknowledgments

This work was supported by the U.S. Department of Energy under contract DE AC04-76-DP 00789.

References

1. E. Conrad, in Digest of Technical Papers from the Third IEEE International Pulsed Power Conference, Albuquerque, New Mexico, 1981, p. 1.
2. See articles in Proceedings of Annual Conferences on Nuclear and Space Radiation Effects, published annually in the IEEE Trans. Nucl. Sci.
3. B. Bernstein and I. Smith, IEEE Trans. Nucl. Sci. NS-20, (1973), p. 294.
4. I. Smith, in Proceedings of the International Conference on Energy Storage, Compression and Switching, edited by W. H. Bostich, V. Nardi, O. Zucker, Asti, Italy, (Plenum Press, New York, 1976), p. 15.
5. Ian Smith, Private Communications, Pulse Sciences, Inc., August 1986.
6. K. R. Prestwich, Energy Storage, Compression, and Switching, edited by W. H. Bostick, V. Nardi, and O. S. F. Zucker, Asti, Italy, (Plenum Press, New York, 1976), p. 451.
7. R. B. Miller, An Introduction to the Physics of Intense Charge Particle Beams, (Plenum Press, New York, 1982).
8. T. W. L. Sanford, J. A. Halbleib, J. W. Poukey, and T. P. Wright, "Theoretical Motivation of Indented-Anode Diode for Hermes III," SAND85-2383 (Albuquerque, NM: Sandia National Laboratories, January 1987).
9. J. J. Ramirez, D. E. Hasti, J. P. Corley, J. W. Poukey, and K. R. Prestwich, "Four-Stage Helia Experiments," in Digest of Technical Papers, 5th IEEE Pulsed Power Conference, Arlington, Virginia, June 1985, p. 143.
10. J. M. Wilson and R. R. Johnston, "PBFA-II Energy Storage System Configuration and Characteristics," in Digest of Technical Papers, 5th IEEE Pulsed Power Conference, Arlington, Virginia, June 1985, p. 776.
11. T. H. Martin, IEEE Trans. Nucl. Sci., NS-20, 3 (1973), p. 289.
12. G. B. Frazier, J. Vac. Sci. Technol. 12, 6 (1975).
13. J. D. Shipman, Jr., IEEE Trans. Nucl. Sci., NS-18, 4 (1971), p. 243.
14. A. R. Miller, in Digest of Technical Papers of the Third IEEE International Pulsed Power Conference, Albuquerque, New Mexico, 1981, p. 200.
15. A. R. Miller, in Digest of Technical Papers of the Fourth IEEE Pulsed Power Conference, Albuquerque, New Mexico, 1983, p. 594.
16. D. L. Johnson, J. P. VanDevender, and T. H. Martin, IEEE Trans. Nucl. Sci. PS-8, 3 (1980), p. 204.
17. T. H. Martin, D. L. Johnson, and D. H. McDaniel, in Proceedings of the Second International Topical Conference on High Pulse Power Electron and Ion Beam Research and Technology, Ithaca, New York, 1977, p. 807.
18. P. Sincerny, D. Strachan, G. Frazier, C. Gilman, H. Helava, S. Wong, J. Banister, T. DaSilva, S. K. Lam, D. LePell, J. Levine, R. Rodenburg, and T. Sheridan, "Performance of Double-EAGLE," in Digest of Technical Papers of IEEE Pulsed Power Conference, Arlington, Virginia, June 1985, p. 151.
19. G. B. Frazier et al., in Digest of Technical Papers of the Fourth IEEE International Pulsed Power Conference, Albuquerque, New Mexico, 1983, p. 583.
20. J. P. VanDevender and T. H. Martin, IEEE Trans. Nucl. Sci., NS-22, 3 (1975), p. 979.
21. T. H. Martin et al., IEEE Trans. Nucl. Sci. NS-28, (1981), p. 3365.
22. C. R. McClenahan, T. P. Wright, J. P. Quintenz, R. C. Backstrom, and P. W. Spence, "Triaxial Diode on HydraMite," SAND85-0740 (Albuquerque, NM: Sandia National Laboratories, October 1985).